MULTI-SCALE LINE DETECTION FOR LANDSLIDE FISSURE MAPPING

André Stumpf [a, b, c], *Thomas A. Lampert* [d], *Jean-Philippe Malet* [b], *Norman Kerle* [c]

[a] Laboratoire Image, Ville, Environnement, CNRS ERL 7230, Université de Strasbourg, 3 rue de l'Argonne, F- 67083 Strasbourg, France
[b] Institut de Physique du Globe de Strasbourg, CNRS UMR 7516, Université de Strasbourg / EOST, 5 rue René Descartes, F-67084 Strasbourg, France
[c] ITC-Faculty of Geo-Information Science and Earth Observation, University of Twente, Department of Earth Systems Analysis, Hengelosestraat 99, P.O. Box 6, Enschede, 7500 AA, The Netherlands
[d] Image Sciences, Computer Sciences and Remote Sensing Laboratory, CNRS UMR 7005, Université de Strasbourg, Bd Sébastien Brant - BP 10413, F-67412 Illkirch, France

1. INTRODUCTION

Surface discontinuities observed in rocks and sediments have proven to be valuable indicators of the deformation history and stress pattern of slopes. For landslide analysis, their observation and interpretation can contribute to a better understanding of the controlling physical processes and help in the assessment of the related hazards [1, 2]. Surface fissures may indicate the development of future failures [3-5] and are often considered as a geo-indicator of the activity stage of a landslide. In sediments, the surface fissure characteristics also influences water infiltration and drainage, which in turn affect the ground-water system and the kinematic response of slopes to hydrological events [6].

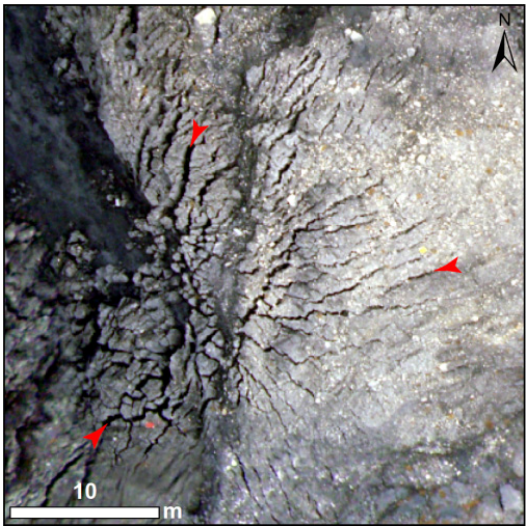

Fig. 1: Test subset of the UAV image with fissures of different sizes marked exemplarily (red arrows).

Recent studies [7] have shown that VHR images acquired from Unmanned Aerial Vehicles (UAVs) are cost-efficient data sources for the monitoring of landslide surfaces at spatial resolutions that allow the recognition of surface features at sub-decimeter scale. Although, the detection and extraction of linear features is a fundamental operation in digital image processing [8, 9] relatively few studies have explored the application of automatic approaches for the mapping of such geomorphological relevant features [10-12].

Considering the increasingly widespread availability of sub-decimetre resolution images from UAVs and other airborne platforms, this study targeted the development of a largely automated image analysis technique to detect landslide surface fissures from VHR aerial images. The developed method is based on scalable Gaussian directional filters that can be used at a single scale or with combined responses over multiple scales. The approach was tested on a multi-temporal VHR images acquired at the Super-Sauze landslide in the Southeast French Alps and the obtained results were compared to manual mappings carried out by experts.

2. DATA AND METHODS

The study site is the slow-moving Super-Sauze landslide located in the Southern French Alps. In October 2010 conducted an aerial survey using a low-cost UAV system at flight heights between 100 and 250 m has been conducted. The image acquisition and processing is detailed in [7]. For this study, a 35 x 35 m subset of the image (Fig. 1) was adopted and the results of the automatic detection were compared with fissure maps elaborated by experts.

The pixel size of the image is 0.08m. The fissures appear as dark curvey-linear features which are 1-10 pixels wide and feature cross profiles that resemble an inverted Gaussian distribution. Following earlier works that exploited such properties for the detection of retinal blood vessels [13, 14] a detection routine using a Gaussian matched filter (GMF) in combination with the first derivate of a Gaussian (FDOG) was implemented.

The GMF is a two dimensional kernel with a zero mean defined in the x-direction by an inverted Gaussian profile (Fig. 2a), and in the y-direction by replicates of the same profile (Fig. 2b). The size of the kernel and corresponding weights are controlled by the standard deviation σ of a constituting Gaussian function defined for $|x| \leq 3\sigma$ and $|y| \leq L/2$. The parameters σ and L therefore adjust the filter's width and length to the width and length of the targeted feature, respectively.

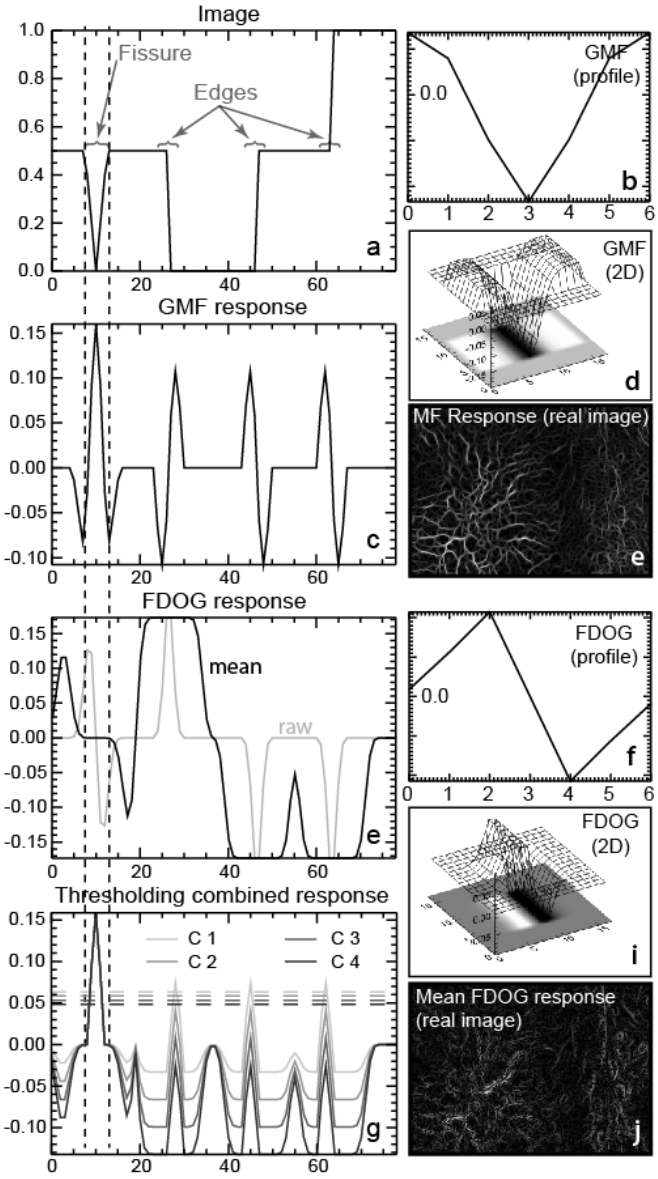

Fig. 2: Illustration of the principles of the Gaussian filtering for a simplified 1-D case (a-c, f-h), a 3D visualization of 2D filters (d,i) and the filter responses on sample image patches.

The length parameter was kept constant at 12 pixels corresponding to a typical fissure length of

As illustrated in Fig. 2c, the GMF yields spurious responses at step edges. This issue can be addressed using an FDOG kernel with the same parameters σ and L (Fig. 2f, i). As illustrated in Fig. 2e the FDOG filter responses with zero crossing at the location of the fissures. When smoothed with a mean filter of the same size as the kernel the zero crossing yields a plateau with low values for the extent of the fissures. Subtracting the absolute values of the smoothed FDOG response from the GMF response yields the final filter output in which responses are suppressed at step edges (Fig. 2g). For a stronger suppression of edge response multiples of the FDOG response

may be subtracted and the final output can be transferred into a binary response selecting a threshold according the desired detection sensitivity. Since in practice the orientation of the fissures is *a priori* unknown, multiple rotated versions of the Gaussian filters are applied on the image and for each pixel only the maximum response value is retained. This corresponds to finding the angle $\theta_{max(x,y)}$ which maximizes the filter response at a given position in the image $I_{(x,y)}$ using Eq. 1:

$$\theta_{\max(x,y)} = \arg\max\left(I_{(x,y)} \otimes GMF_{\theta i}\right), \qquad \text{for } 0 < \theta_i \leq \pi,\ i = \{1,2,\dots 36\} \qquad \text{Eq. 1}$$

where $\otimes$ denotes the convolution operator and θ_i the orientation of the GMF. The observed variability of the fissure width also suggests a search among multiple scales and it has been demonstrated that the family of Gaussian filters provides an adequate frame work for scale-space analysis [15]. According to scale-space theory the Gaussian filter will yield a maximum response as it approaches the scale of a target feature present in the image. Applying the filter among a number of predefined scales and retaining for each pixel only the maximum response this property can be can be used for automatic scale selection, as recently demonstrated for line detection applications [16]. This is similar to finding the orientation of the fissure and is expressed in Eq. 2:

$$\sigma_{\max(x,y)} = \arg\max\left(I_{(x,y)} \otimes GMF_{\sigma i}\right), \qquad \text{for } \sigma_i = \{0.6, 0.8, \dots 3.0\} \qquad \text{Eq. 2}$$

In summary, for each pixel the algorithm finds the GMF peak response orientation and scale, calculates the smoothed response of a corresponding FDOG at the same orientation and scale and subtracts the FDOG from the GMF. All detections were performed on the green band of the image.

3. RESULTS AND DISCUSSION

Receiver operating characteristic (ROC) analysis is a frequently adopted technique to assess the performance of feature detection algorithms since it is not affected by class-imbalance and allows a threshold independent comparison among different algorithms [17]. An ROC analysis was carried out to assess the performance of the multi-scale fissure detection with respect to two expert maps and compare the results with the single-scale method. The ROC plots in Fig. 3d and 3h illustrate that in most cases the multi-scale algorithms outperforms the single scale detector, whereas with more conservative thresholds and ground truth (Fig. 3g) the single scale detector with the smallest $\sigma=0.6$ still yielded lower false positive rates. This must be attributed to generally broader responses resulting from peak responses at larger scales in the multi-scale detection.

In addition to competitive detection accuracies, the proposed algorithm liberates the user from an exhaustive search over all possible scales and appears especially useful in situations where the targeted features exhibit great size variability. A comparison of the manual mappings (Fig. 3 c, g) also reveals the uncertainty of the reference data, which is typical among the ground truth maps based on expert judgments. However, the fact that the inter-observer agreement is still above the accuracy of the automated detection also indicates that objective image information is still not fully exploited and further enhancements to the technique are possible.

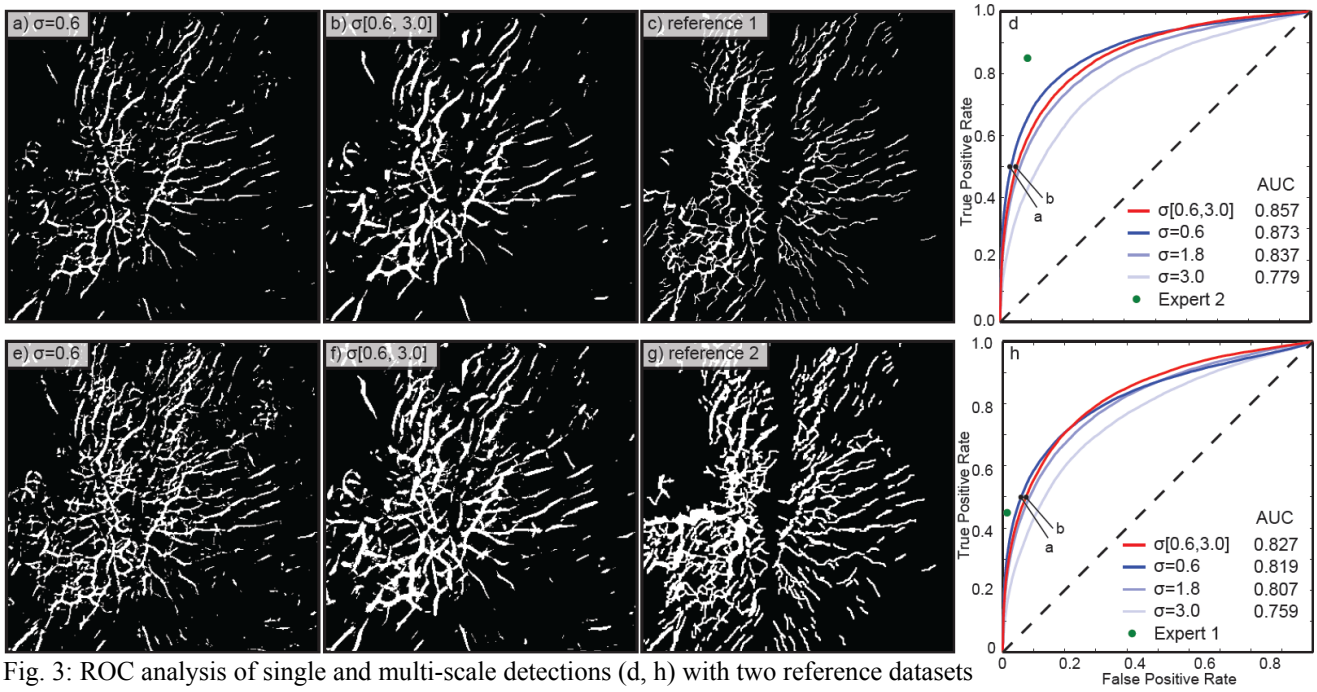

Fig. 3: ROC analysis of single and multi-scale detections (d, h) with two reference datasets (c, g). The best detection results are displayed at a true positive rate of 0.5 (a, b, e, f).

4. REFERENCES

[1] R. W. Fleming and A. M. Johnson, "Structures associated with strike-slip faults that bound landslide elements," *Engineering Geology,* vol. 27, pp. 39-114, 1989.

[2] M. Parise, "Observation of surface features on an active landslide, and implications for understanding its history of movement," *Nat. Hazards Earth Syst. Sci.,* vol. 3, pp. 569-580, 2003.

[3] R. N. Chowdhury and S. Zhang, "Tension cracks and slope failure. ," presented at the International Conference In Slope Stability Engineering: developments and applications. Proceedings of an international conference, Isle of Wight, 1991

[4] G. A. Khattak, L. A. Owen, U. Kamp, and E. L. Harp, "Evolution of earthquake-triggered landslides in the Kashmir Himalaya, northern Pakistan," *Geomorphology,* vol. 115, pp. 102-108, 2010.

[5] K. B. Krauskopf, S. Feitler, A. B. Griggs, and Source:, "Structural Features of a Landslide near Gilroy, California," *The Journal of Geology,* vol. 47, pp. 630-648, 1939.

[6] J. P. Malet, T. W. J. van Asch, R. van Beek, and O. Maquaire, "Forecasting the behaviour of complex landslides with a spatially distributed hydrological model," *Nat. Hazards Earth Syst. Sci.,* vol. 5, pp. 71-85, 2005.

[7] U. Niethammer, M. R. James, S. Rothmund, J. Travelletti, and M. Joswig, "UAV-based remote sensing of the Super-Sauze landslide: Evaluation and results," *Engineering Geology,* vol. In Press, Accepted Manuscript, 2011.

[8] L. J. Quackenbush, "A review of techniques for extracting linear features from imagery," *Photogrammetric Engineering & Remote Sensing,* vol. 70, pp. 1383–1392, 2004.

[9] G. Papari and N. Petkov, "Edge and line oriented contour detection: State of the art," *Image and Vision Computing,* vol. 29, pp. 79-103, 2011.

[10] B. V. M. Shruthi, N. Kerle, and V. Jetten, "Object-based gully feature extraction using high resolution imagery," *Geomorphology,* in press.

[11] A. Baruch and S. Filin, "Detection of gullies in roughly textured terrain using airborne laser scanning data," *ISPRS Journal of Photogrammetry and Remote Sensing,* vol. 66, pp. 564-578, 2011.

[12] A. Stumpf, U. Niethammer, S. Rothmund, A. Mathieu, J.-P. Malet, N. Kerle, and M. Joswig, "Advanced image analysis for automated mapping of landslide surface fissures," presented at the 2nd World Landslide Forum, Rome, Italy, 2011.

[13] S. Chaudhuri, S. Chatterjee, N. Katz, M. Nelson, and M. Goldbaum, "Detection of blood vessels in retinal images using two-dimensional matched filters," *Medical Imaging, IEEE Transactions on,* vol. 8, pp. 263-269, 1989.

[14] B. Zhang, L. Zhang, L. Zhang, and F. Karray, "Retinal vessel extraction by matched filter with first-order derivative of Gaussian," *Computers in Biology and Medicine,* vol. 40, pp. 438-445, 2010.

[15] T. Lindeberg, "Feature Detection with Automatic Scale Selection," *International Journal of Computer Vision,* vol. 30, pp. 79–116, 1998.

[16] T. A. Lampert and S. E. M. O'Keefe, "A detailed investigation into low-level feature detection in spectrogram images," *Pattern Recognition,* vol. 44, pp. 2076-2092, 2011.

[17] T. Fawcett, "An introduction to ROC analysis," *Pattern Recogn. Lett.,* vol. 27, pp. 861-874, 2006.